Laser Induced Modifications of Carbon Nanotube Composite Surfaces

Ayman Bassil, Pascal Puech, Wolfgang Bacsa, P. S. Pizani, R. G. Jasinevicius, Philippe Demont, Sophie Barrau, Colette Lacabanne, Revathi Bacsa, Emmanuel Flahaut

Laser Induced Modifications of Carbon Nanotube Composite Surfaces

A. BASSIL*, P. PUECH, W. BACSA, P. S. PIZANI[1], R. G. JASINEVICIUS[2], Ph. DEMONT[3], S. BARRAU[3], C. LACABANNE[3], R. BACSA[4] and E. FLAHAUT[4]

LPST, IRSAMC, UMR5477, Université Paul Sabatier, 31062 Toulouse Cedex 4, France
[1]*Departamento de física, universidade Federal de São-Carlos, C.P. 369, 13560-970 São-Carlos, SP, Brazil*
[2]*Departamento de Engenharia Mecânica, Escola de Engenharia de São Carlos, Universidade de Sao Paulo, CP359, CEP 13560-970, São Carlos, SP, Brazil*
[3]*LPP, CIRIMAT, UMR5085, Université Paul Sabatier, 31062 Toulouse Cedex 4, France*
[4]*LCMIE, CIRIMAT, UMR5085, Université Paul Sabatier, 31062 Toulouse Cedex 4, France*

Carbon nanotubes epoxy composites have been processed with high power laser pulses and micro-machined with a single crystal diamond tool. The effect of the dispersion of the carbon nanotubes (CNTs, 0.4 wt %) in the epoxy resin and carbon nanotube interaction with the composite matrix have been probed using spectroscopic Raman mapping. While the micro-machined surface maintains a good electrical conductivity after machining, the surface is poorly conductive after laser ablation. Laser processing (power 150 J/pulse, 1064 nm) transforms the surface of the carbon nanotube nanocomposite up to a distance of 25 µm. AFM images show that the diamond machined surface reduces the composite surface roughness.
[DOI: 10.1143/JJAP.45.7776

KEYWORDS: nanotubes, composites, Raman spectroscopy, laser processing, machining

1. Introduction

Carbon nanotubes (CNTs) have received considerable attention due to their remarkable mechanical properties,[1,2] high electrical,[3] and thermal conductivity.[4,5] This makes them attractive to improve the electrical and mechanical properties of composites.[6–10] Micro machining is often used to test and study the mechanical properties of materials and to reduce the surface roughness. The surface morphology is an important parameter for the application of CNT composites. Factors which influence their performance are surface roughness, microstructure and residual stress, micro hardness apart of electrical and thermal conductivity. Laser processing is widely used to machine a variety of materials. The thermal properties of the target, is particularly important in the performance of the process. Pulsed laser ablation on graphite[11,12] have been reported showing a transformed zone of tens of micrometers around the formed craters. Adding CNTs in epoxy has the effect of increasing the electrical conductivity at low filling due to the low percolation threshold for nanotubes (0.4% CNT).[13] Full understanding of CNT interaction with the epoxy matrix has been an important issue for applications in aeronautics industry. Not much attention has been given so far on the changes of the CNT composite surface induced by industrial processing methods. Raman scattering is non destructive and a relative simple tool to study the structure and electronic properties of CNTs.[14] The spectrum of CNT is sensitive to the tube environment. Raman mapping of carbon nanotube epoxy resin (CNT-ER) can be used as a diagnostic tool to get information of the CNT dispersion and their interaction with the composite matrix.[15] CNTs have been proposed as molecular stress sensors due to their high spectroscopic sensitivity to their environment.[16,17] In this paper we report on Raman spectroscopic and electrical conductivity measurements on micro machined and laser processed CNT composites.

*E-mail address: ayman.bassil@lpst.ups-tlse.fr

2. Experimental Procedure

The CNTs were prepared by the catalytic chemical vapor deposition method (CCVD). Selective reduction at 1000 °C in a methane–hydrogen (18% CH_4) atmosphere of a solid solution of a transition metal oxide $Mg_{0.95}Co_{0.05}$ led to the formation of small diameter CNTs with one to three walls (for more details see refs. 13–18). After the reaction, the unreacted catalytic particles were dissolved in dilute (3.7%) hydrochloric acid and CNTs were recovered. High-resolution electron microscopy images show the presence of individual CNTs and small bundles of CNTs with an average diameter of 2.4 nm. The nanotubes were mainly single (SW) and double walled (DW). A dispersion of CNTs in water was first kept in an ultrasonic bath for 1 h and stirred. No surfactants were used. CNT epoxy resin composites were prepared by dispersion of weight amount of CNTs ranging from 0.04 to 0.4 wt %. The liquid epoxy resin was added to the dilute suspension of nanotubes and water was evaporated at 100 °C. The mixture was then mechanically stirred for 1 h at 2000 rpm. The hardener was added and the whole mixture was mechanically stirred for 15 min and then cast into a Teflon mould and degassed for 20 min under vacuum. The nanocomposite was cured at 120 °C for 20 min and at 145 °C for another 8 h. The effect of micro-machining and laser irradiation is studied using a concentration of 0.4 wt % CNTs, a value slightly above the bulk electrical percolation threshold. All Raman spectra were recorded at room temperature (MicroRaman, Renishaw Inc). The scattered light was collected in backscattering geometry using a microscope objective (40x, numerical aperture 0.4) to focus the laser beam (514 nm) on the sample. Laser irradiation studies were performed using a YAG laser (100 W, 1063 nm) with 0.8 ms long pulses (150 J) and 0.15 mm beam diameter. Single-point diamond turning tests were carried out on a commercially available ultra-precision diamond turning machine, the Aspheric Surface Generator Rank Pneumo ASG 2500. The surface of the CNT composite was face turned with a round nose (radius of 1.5 mm) single crystal diamond tool (Contour Fine Tooling®). The cross-feed

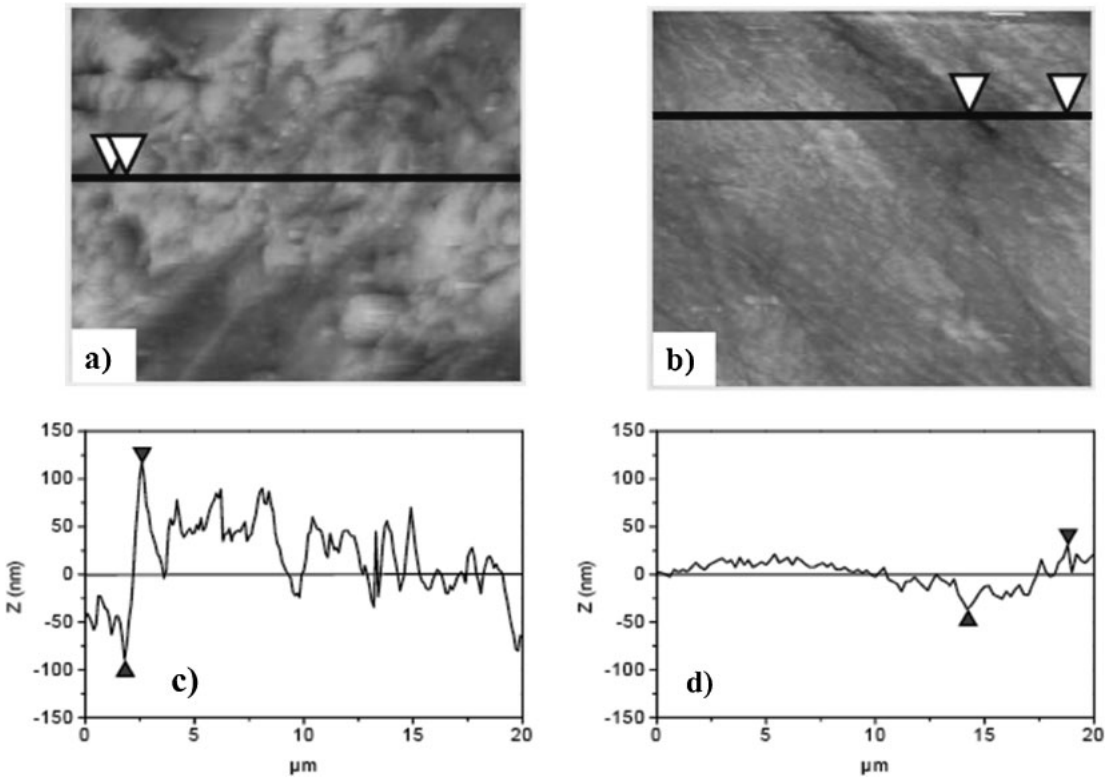

Fig. 1. Scanning force microscope images (size: 20 μm) of CNT–epoxy resin composite on non machined surface (a), machined surface (b); (c) and (d) show the roughness of non machined and machined surface respectively.

direction was outside to inside. The geometry of the cutting tool was 0° rake angle and a clearance angle of 12°. No cutting fluid was used with the purpose of cooling or lubrication since the CNT composite material is soft. The feed rate and depth of cut applied in the cutting tests were 10 μm/rev. The spindle speed was kept constant at 1000 rpm. The test provided ductile mode machining which results in a smooth surface finish. The AFM images were measured using a Digital Instruments NanoScope IIIa instrument at normal condition (air, 25 °C). The conductivity measurements were carried out by recording the complex conductivity $\sigma^*(\omega)$ using a Solartron-Schlumberger frequency response analyzer together with a Novocontrol interface. The measurements were carried in the frequency range between 10^{-2} and 10^6 Hz at room temperature. The real part, $\sigma'(\omega)$, of the complex conductivity $\sigma^*(\omega)$ was investigated. For the dc conductivity σ_{dc} we have taken the value of $\sigma'(\omega)$ at 10^{-2} Hz.

3. Results and Discussion

Figure 1 shows scanning force microscope images (AFM) (20 μm) of the CNT composite before (a) and after machining the surface (b). Line-scans are shown of the two surfaces in (c) and (d). The triangular marks in Figs. 1(a) and 1(b) indicate the highest and lowest point of the surface in Z direction perpendicular to the scanned surface to show the maximum height variation apart of the surface roughness. The measured mean roughness value is 3 nm for the machined surface and 54 nm for non machined surface respectively. The CNT epoxy resin composite was laser processed using a pulse time of 0.8 ms and pulse energy of 150 J using the 1064 nm laser excitation.

Figure 2 shows Raman maps of the G-band position across regions on three faces of the sample: non treated surface [Fig. 2(a)], micro-machined surface [Fig. 2(b)] and laser irradiated surface [Fig. 2(c)]. The G-band position has been determined by fitting the peak to a single Lorentzian line shape. We observe a large variation (20 cm^{-1}) of the G band position across the surface in Figs. 2(a) and 2(b) which we attribute to the different environment of the CNTs in the epoxy resin. The G band is sensitive to pressure and shifts to higher frequency with increasing pressure.[14] The continuous variation of the G band from 1590 to 1610 cm^{-1} is attributed to local pressure variations in the neighbourhood of the CNT. The shape of the G band of SWCNT and DWCNT is different from MWCNT. We notice that the D′ band, sensitive to the presence of defects, is located in the same frequency range and is observed when the G band is located at 1580 cm^{-1}. The small D to G band intensity ratio indicates clearly that no breaking of DWNTs in the epoxy matrix takes place. We notice that DWNTs need grinding, using ball milling, for more than 24 h to break the tubes.

In the case of the laser irradiated surface no Raman G-band is observed at all and we conclude that the CNTs are not present in the surface region after laser irradiation. Using the wavelength and the numerical aperture of the microscope objective we can estimate a light penetration length of 7 μm. The brighter regions in Figs. 2(a) and 2(b) correspond to large G-band shifts and are associated with the regions of the surface where the CNT are in contact with the polymer matrix and are well dispersed.[15] The darker regions in Figs. 2(a) and 2(b) correspond to G-band shifts observed for DWNTs without the polymer matrix. We attribute these

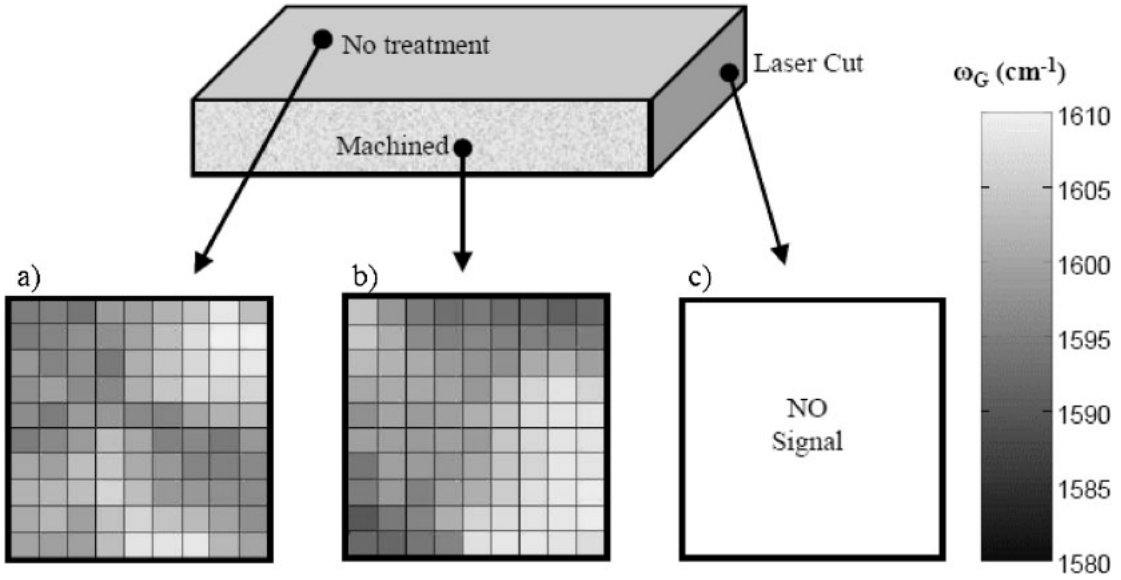

Fig. 2. Raman map ($50 \times 45\,\mu m^2$, step size: $5\,\mu m$) of G-band position with (a) not machined, (b) machined and (c) laser irradiated surface of the CNT–epoxy resin composite.

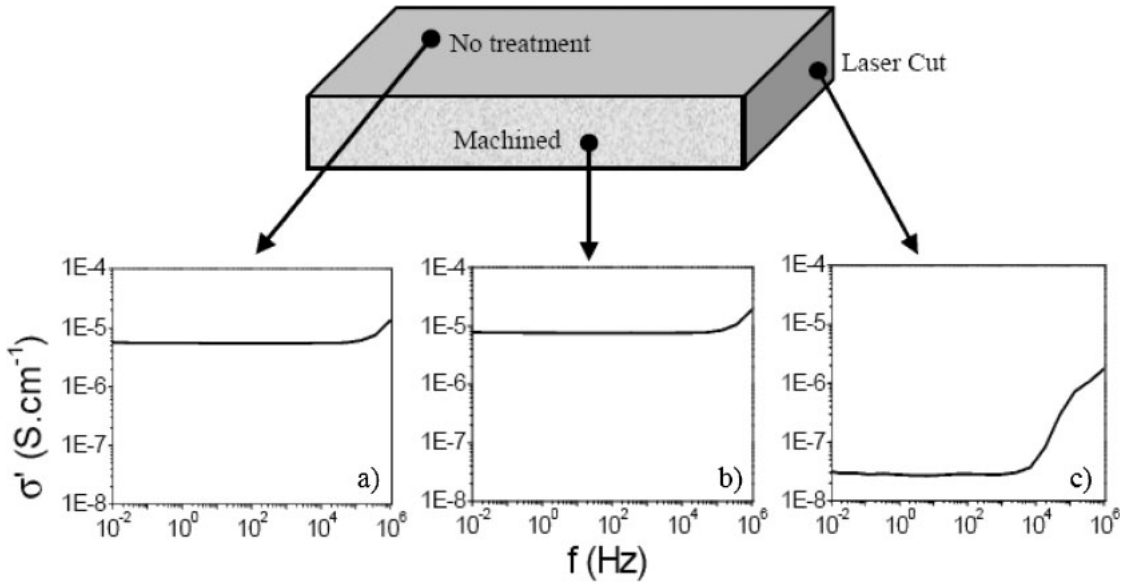

Fig. 3. Frequency dependence of the real part of the complex conductivity $\sigma'(\omega)$ for (a) not machined, (b) machined and (c) laser irradiated surface of the CNT–epoxy resin composite.

regions to areas where the CNTs are agglomerated and are not in contact with the polymer matrix, except for the tubes at the interface between the agglomerate and the polymer matrix. We conclude that by mapping the G-band on polymer composite surfaces it becomes then possible to assess the CNT dispersion in the composite surface region. Interestingly no G-band has been observed for the laser processed surface in Fig. 2(c). This indicates that the absorbed heat from the laser pulse, mostly absorbed by the CNTs, has the effect of removing the tubes from the surface region. The CNTs are pulled into the polymer matrix or oxidized.

Figure 3 shows the ac conductivity (10^{-2}–10^{6} Hz, 25 °C). For the dc conductivity σ_{dc} we have taken the value of the ac conductivity at the lowest measured frequency (10^{-2} Hz) for both machined and irradiated samples. The dc conductivity value of the pristine epoxy resin is at the level of 8×10^{-16} S·cm^{-1}. The addition of 0.4% of CNT increases the dc conductivity by 10 orders of magnitude to reach 10^{-6} S·cm^{-1}. From the frequency dependence of the real part $\sigma'(\omega)$ of the complex electrical conductivity $\sigma^*(\omega)$ we find that the machined and not machined composites have the same conductivity of about 10^{-6} S·cm^{-1} and the bulk conductivity of the laser irradiated composite is reduced to by two orders of magnitude to 10^{-8} S·cm^{-1}. This is compatible with the Raman maps which show that CNTs are absent in the surface region. We conclude that the mechanical machining does not reduce the conductivity of the CNT composite but increases the electrical conductivity by 40%. The higher surface flatness improves the electrical contact with the gold-plated brass electrodes (diameter of 1 cm).

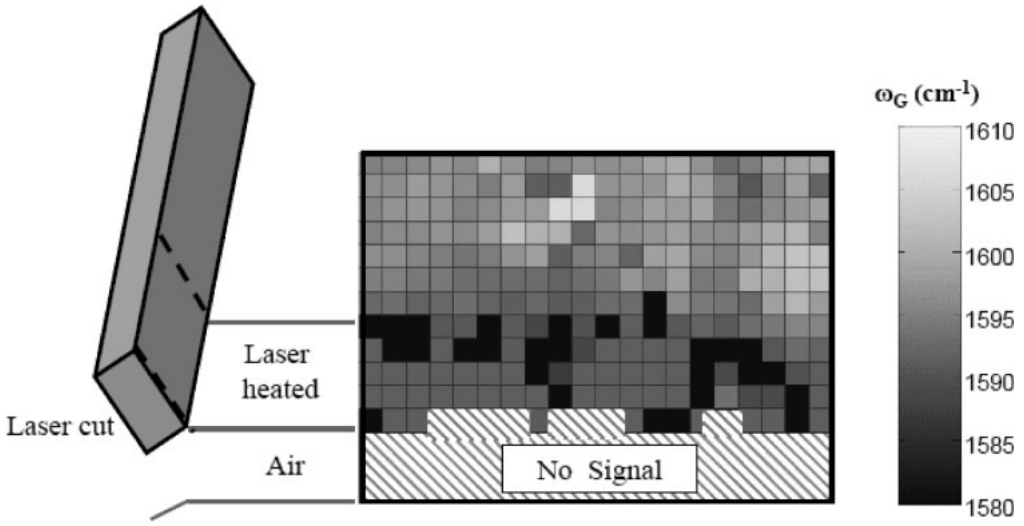

Fig. 4. Raman map ($100 \times 75\,\mu m^2$, step size $5\,\mu m$) of the G-band position in a plane perpendicular to the laser irradiated surface.

Figure 4 shows a $100 \times 75\,\mu m^2$ Raman map of the laser machined CNT composite in a plane perpendicular to the laser irradiated surface. Three zones can be identified: the first zone, near the laser irradiated surface where no G band is observed, the second zone where the position of the G-band is always lower than $1590\,cm^{-1}$ and a third zone at a distance $>25\,\mu m$ from the laser irradiated surface where the G band shifts are larger than $1590\,cm^{-1}$. We can conclude that CNTs are not well dispersed in the resin epoxy resin matrix near the laser irradiated surface within a distance of at least $25\,\mu m$ from the surface. Carbon nanotubes are good absorbers at 1064 nm. Their exceptionally high thermal conductivity[5,20,21] and chemical stability[22] (about 500 °C in air) has the effect that the absorbed thermal energy from the laser pulse heats the CNTs in the epoxy matrix selectively. This has the effect of preserving bundling and agglomeration of tubes and reducing the interaction with the polymer matrix and removing the CNTs from the intermediate surface region. The presence of oxygen and the release of singlet oxygen from the epoxy matrix are expected to burn CNTs. At larger distances from the surface the absorbed heat and the induced agglomeration is reduced. Laser irradiation of CNT epoxy composites can then be used to reduce locally the electrical conductivity which might be useful for applications where certain parts of the surface need to be electrically isolated.

4. Conclusions

While the surface of laser processed CNT epoxy composites affect strongly the ac conductivity, we find that micro machining of CNT epoxy increases the ac conductivity by 40%. AFM surface profiling shows a clear improvement of the surface roughness for micro-machined composite surfaces. Laser irradiation of CNT nanocomposites removes the CNTs from the surface region within a depth of $25\,\mu m$. Selective optical absorption of CNTs has the effect that CNTs are pulled into the epoxy matrix or oxidized and removed from the surface.

1) A. Bachtold, P. Hadley, T. Nakanishi and C. Dekker: Science **294** (2001) 1317.
2) A. Hashimoto, K. Suenaga, A. Gloter, K. Urita and S. Ijima: Nature **430** (2004) 870.
3) T. W. Ebbesen, H. J. Lezec, H. Hiura, J. W. Bennett, H. F. Ghaemi and T. Thio: Nature **382** (1996) 54.
4) J. Hone, M. Whitney, C. Piskoti and A. Zettl: Phys. Rev. B **59** (1999) R2154.
5) S. Berber, Y. K. Kwon and D. Tomanek: Phys. Rev. Lett. **84** (2000) 4613.
6) J. C. Kearns and R. L. Shambaugh: J. Appl. Polym. Sci. **86** (2002) 2079.
7) E. S. Choi, J. S. Brooks, D. L. Eaton, M. S. Al-Haik, M. Y. Hussaini, H. Garmestani, D. Li and K. Dahmen: J. Appl. Phys. **94** (2003) 6034.
8) B. Kim, J. Lee and I. Yu: J. Appl. Phys. **94** (2003) 6724.
9) D. Shi, J. Lian, P. He, L. M. Wang, F. Xiao, L. Yang, M. J. Schulz and D. B. Mast: Appl. Phys. Lett. **83** (2003) 5301.
10) M. Cadek, J. N. Coleman, K. P. Ryan, V. Nicolosi, G. Bister, A. Fonseca, J. B. Nagy, K. Szostak, F. Beguin and W. J. Blau: Nano Lett. **4** (2004) 353.
11) M. Bonelli, A. Miotello, P. M. Ossi, A. Pessi and S. Gialanella: Phys. Rev. B **59** (1999) 21.
12) M. D. Shirk and P. A. Molian: Carbon **39** (2001) 1183.
13) S. Barrau, Ph. Demont, A. Peigney, Ch. Laurent and C. Lacabane: Macromolecules **36** (2003) 5187.
14) S. Ijima: Nature (London) **354** (1991) 56.
15) A. Bassil, P. Puech, G. Landa, W. Bacsa, S. Barrau, P. Demont, C. Lacabanne, R. Bacsa, E. Flahaut, A. Peigney, C. Laurent and E. Perez: J. Appl. Phys. **97** (2005) 034303.
16) J. R. Wood and H. D. Wagner: Appl. Phys. Lett. **76** (2000) 2883.
17) L. S. Schadler, S. C. Giannaris and P. M. Ajayan: Appl. Phys. Lett. **73** (1998) 3842.
18) E. Flahaut, A. Peigney, C. Laurent and A. Rousset: J. Mater. Chem. **10** (2000) 249.
19) R. Bacsa, Ch. Laurent, A. Peigney, W. Bacsa, T. Vaugien and A. Rousset: Chem. Phys. Lett. **323** (2000) 526.
20) P. Kim, L. Shi, A. Majmudar and P. L. McEuen: Phys. Rev. Lett. **87** (2001) 215502.
21) E. Pop, D. Mann, Q. Wang, K. Goodson and H. Dai: Nano Lett. **6** (2006) 96.
22) X. LU, K. D. Ausman, R. D. Piner and R. S. Ruoff: J. Appl. Phys. **86** (1999) 186.